SOLAR ENERGY CONTRIBUTION TO THE ENERGY DEMAND FOR AIR CONDITIONING SYSTEM IN AN OFFICE BUILDING UNDER TRIPOLI CLIMATE CONDITIONS

by

Mohamed H. MUSBAH*[*], *Branislav D. ŽIVKOVIĆ, Franc F. KOSI, Mohamed M. ABDULGALIL, and Aleksandra A. SRETENOVIĆ

Faculty of Mechanical Engineering, University of Belgrade, Belgrade, Serbia

Original scientific paper
DOI: 10.2298/TSCI121229124M

The feasibility of solar assisted air-conditioning in an office building under Tripoli weather conditions is investigated in this paper. A single-effect lithium bromide absorption cycle powered by means of flat-plate solar collectors was modeled in order to predict the potential of the solar energy share. The cooling load profile was generated by using a detailed hourly based program and typical meteorological year for Tripoli. System performance and solar energy fraction were calculated by varying two major parameters (collector's slope angle and collector area).The maximum solar fraction of 48% was obtained by means of 1400 m^2 of collector surface area. Analysis of results showed that, besides the collector surface area, the main factors affecting the solar fraction were the local weather conditions (intensity of incident solar radiation) and the time of day when the plant was operated.

Key words: *solar energy, absorption system, office building, cooling load, energy consumptions*

Introduction

Air-conditioning and dehumidification are the dominating energy consuming services in both residential and commercial buildings during the summer in Libya. According to Libyan energy providers and government organization, Libya's electric energy demand is expected to double by 2014, and it will be more than two and a half times by the end of the year 2020[1]. This rising demand for electricity causes the increase in fossil fuel consumption, which results in an increase of CO_2 emission, and threatens the stability of electricity supply. Thus, replacement of a conventional cooling system based on fossil fuels by solar cooling technology to cover the cooling load, seems to be one of the most attractive solutions, since the seasonal cooling loads coincide with high intensity of solar radiation.

The basic idea of solar air-conditioning technologies is the utilization of heat driven cooling machines (absorption system) in combination with solar thermal energy systems to produce the cooling effect. A variety of solar collectors are used as a heat source for both heating systems or thermally driven refrigeration processes worldwide [2,3]. For air-conditioning systems, it is common to use chilled water temperature 5-7 °C for cooling and dehumidification purpose which is achievable with single-effect absorption machines, and it fits to apply solar energy in air-conditioning for office and commercial buildings [4].

[*] Corresponding author, e-mail: m.hadyia@hotmail.com

Balghouthi *et al.* [5] have studied the feasibility of solar-powered absorption cooling technology for a residential building under Tunisian conditions. The system was modeled using the TRNSYS and EES programs with a meteorological year data for Tunis, the capital of Tunisia. The optimized system for a typical building of 150 m^2consisted of a $LiBr/H_2O$ absorption chiller with a capacity of 11 kW, a 30 m^2 flat-plate solar collector area tilted at 35° from the horizontal, and a 0.8 m^3 hot water storage tank.

Elsafty and Al-Daini [6] made an economic comparison of the solar-powered single/double effect vapor absorption air-conditioning system and a vapor compression system using the present worth comparison method and equivalent annual comparison method. The analysis was made in order to select the appropriate air conditioning system that could satisfy 879 kW of cooling load for the Students hospital in Alexandria, Egypt. The interrelationship between economic and thermodynamic aspects was also considered, such as the dependence of operating costs on the surrounding climatic conditions.

Mazloumi *et al.* [7] simulated a single-effect absorption cooling system designed to supply the cooling load of a typical house in Ahwaz where the cooling load peak was about 17.5 kW. Solar energy was absorbed by a horizontal N-S parabolic trough collector and stored in an insulated thermal storage tank. It was concluded that the minimum required collector area was about 57.6 m^2, which could eliminate the cooling loads for the sunshine hours of the design day.

In spite of the extensive literature reported and published worldwide regarding solar absorption cooling technology, none of these papers were considering the feasibility of solar absorption cooling system for residential or commercial building under Libyan climatic conditions. This paper bridges this knowledge gap by modeling and analyzing a solar absorption assisted air conditioning system for a typical office building located in Tripoli, Libya. This model is developed using a Math CAD program in order to predict the contribution of solar energy to satisfy the cooling demand of an office building under Tripoli climate zone. A thermal analysis is carried out in order to investigate the influence of the collector surface area and the tilt angle of solar collector on the solar energy contribution. The investigation of these parameters is performed with respect to the solar fraction (SF) and auxiliary heater fraction (AHF).

Description of the proposed system

A solar thermal system and a lithium bromide single-effect absorption system, integrated into one cooling plant to provide the cooling necessity for an office building in Tripoli, Libya (32° 53' N latitude and 13° 10' E longitude)during the cooling season (April – September). Figure 1 presents the general scheme of the integrated plant. The major components of the plant are the roof-mounted flat-plate solar collectors, a 500 kW cooling single-effect $LiBr/H_2O$ absorption chiller, a hot water storage tank, a cold water storage tank, a conventional boiler serving as auxiliary heater, a cooling tower, fan coil units, pumps and some other accessories. There are three water loops (hot water loop, chilled water loop, cooling water loop). The hot water is circulated between the generator and solar collectors, the chilled water is circulated between the evaporator and fan-coil units, and cooling water is circulated through the absorber, the condenser and cooling tower, respectively. This series arrangement of the cooling water loop for both condenser and absorber are applied to avoid the crystallization and to use a single pump, which is easy to control. To ensure a stable operation of the system, an auxiliary heat source is used whenever the solar energy is insufficient to provide the required temperature level needed by the generator [8].

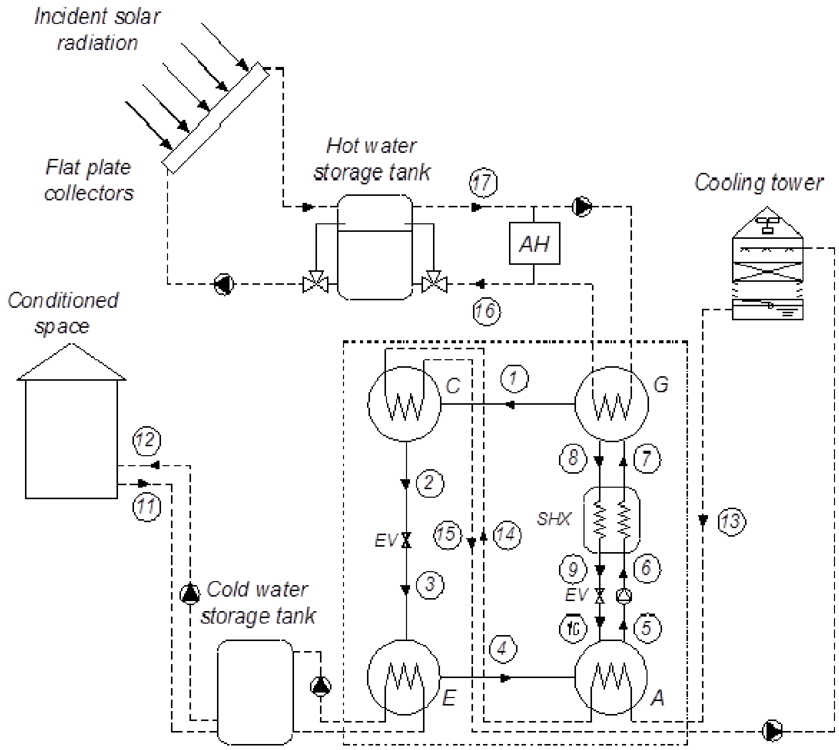

Figure 1.General scheme of a solar-powered single-effect absorption cooling system
generator (G),condenser (C), evaporator (E), absorber (A), solution heat exchanger (SHX), auxiliary heater (AH) and expansion valve (EV)

Building load

A typical office building of rectangular shape is considered to serve as a baseline load reference for our study. The building is oriented towards the north and consists of three floors with 1152 m^2 of floor surface area each and 3.2 m of height. The air conditioning system is designed to satisfy the cooling demand during office hours (from 8 a. m. to 6 p. m.), from Monday to Friday with a cooling set point temperature of 26 °C.

According to Libyan climate, space cooling is required from April to October. Therefore, the cooling season in the model calculation is selected to be from the beginning of April to the end of September. The hourly analysis program is used to estimate the cooling load profile based on the typical meteorological year (TMY) for Tripoli. The cooling load calculation takes into account the occupancy, ventilation, electrical gains, insulation, shading coefficient and building envelope behavior. The space load is classified into sensible and latent heat for the proper selection of air conditioning system. The fresh air requirement is accomplished by the primary air handling unit at a rate of 50 m^3/h per occupant, while the cooling load is handled by the fan coil units. The air handling unit supplies conditioned air to the office building at the constant air flow rate. The variation of the hourly outdoor dry-bulb temperatures and the cooling load profile of the office building corresponding to the 21st of

July are presented in fig. 2. The maximum building load (air conditioning and ventilation) reaches the value of 484 kW on 21st of July at 4 pm.

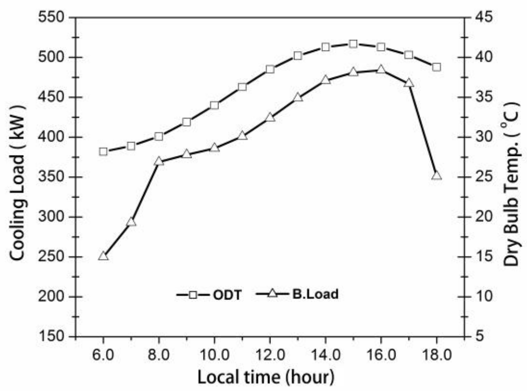

Figure 2.The daily cooling load profile and the design dry-bulb temperature for 21st July

Mathematical model

Solar collector model

There are many types of solar collectors, which are used in air conditioning applications including flat-plate collector, evacuated tube collector and compound parabolic collectors. In our case, the selected type is a flat-plate solar collector due to its relative low cost and ability to make the use of both diffuse and beam components. The base case is equipped with 1000 m^2 of solar collector area, with an aperture area of 2 m^2 for each unit. It's very important to install solar collectors at an optimum orientation in order to maximize the capture of solar radiation by its absorber surfaces. Thus, the collectors are adjusted with an optimum tilt angle of 20° facing south, and used in forced circulation mode with mass flow rate of 0.02 kg/s m^2. Estimating the total intensity of solar energy received by the flat-plate solar collector is a complex function of different parameters such as local climatology patterns, orientation and inclination of the collector surface *etc*. Furthermore, the total solar radiation incident on a tilted surface must be determined by converting the solar radiation measured on a horizontal surface to that incident on the tilted surface of interest in order to design the system size and estimate its performance.

The available solar radiation data, which have been measured by the Libyan meteorological center, are the daily total solar radiation on a horizontal surface. However, it is necessary to estimate the beam and diffuse solar radiation received by the flat-plate collector separately; therefore, the hourly diffuse and beam solar radiation are defined as follows [9,10]:

The monthly average daily extraterrestrial solar irradiance H_0 incident on a surface normal to the Sun's ray can be approximated as following:

$$H_0 = \frac{24 \cdot 3600 \cdot G_{sc}}{\pi} \cdot \left[1 + 0.033\cos\left(\frac{360n}{365}\right)\right] \cdot \left(\cos LAT \cdot \cos\delta \cdot \sin\omega_s + \frac{\pi\omega_s}{180} \cdot \sin LAT \cdot \sin\delta\right) \tag{1}$$

The sunset hour angle is given as:

$$\cos\omega_s = -\frac{\sin LAT \cdot \sin\delta}{\cos LAT \cdot \cos\delta} \tag{2}$$

The daily diffuse solar fraction k_d is evaluated by the sky clearness index k_T, which is defined as:

$$k_T = \frac{H}{H_0} \tag{3}$$

The daily horizontal diffuse radiation H_0 is obtained by the following equation:

$$H_d = k_d \cdot H \tag{4}$$

$$k_d = e^{-0.355+(0.0711 \cdot kT)-(2.51 \cdot kT^2)} \tag{5}$$

The hourly diffuse radiation I_d is then:

$$I_d = \left[\frac{r_d \cdot H_d}{3600}\right] \tag{6}$$

Once the hourly diffuse radiation I_d is determined, the hourly beam radiation I_b is given by:

$$I_b = \frac{H}{\tau} - I_d \tag{7}$$

The total solar irradiation I_m at any orientation and tilt with an incident angle θ is the sum of the direct component to the surface ($I_{DN}\cos\theta$) and the diffuse component I_d coming from the sky plus whatever amount of reflected radiation I_r (neglected) may reach the surface from the earth or from adjacent surfaces. Also it's very important to define the angle of incidence θ which is the angle between the line normal to the aperture of the collector surface and the earth-sun line. Its value is given by:

$$\cos\theta = \cos\beta \cdot \cos\gamma \cdot \sin\Sigma + \sin\beta \cdot \cos\Sigma \tag{8}$$

The total solar radiation I_{tts} on a tilted surface of flat-plate collector is estimated by:

$$I_{tts} = I_{DN} \cdot \cos\theta + I_d \tag{9}$$

The performance of the solar collector is calculated using the theory of Hottel and Whillier presented by Duffie and Beckman [9]. The basic parameter to be considered is the collector thermal efficiency which is defined as the ratio of the useful energy delivered to the total energy incident on the collector area.

$$\eta = \frac{Q_u}{G_t} \tag{10}$$

Under steady-state conditions, the useful heat gain per unit of the collection area is obtained by applying the energy balance that indicates the distribution of incident solar energy into useful heat gain, thermal losses and optical losses, as given in the following equation:

$$Q_u = A_{sc} \cdot FR\left[SR - UL(T_{sol,in} - T_{amb})\right] \tag{11}$$

The heat removal factor is given by:

$$FR = \left(\frac{\dot{m}_f \cdot Cp_f}{A_{sc} \cdot UL}\right) \cdot \left[1 - \exp\left(\frac{UL \cdot A_{sc} \cdot F'}{\dot{m}_f \cdot Cp_f}\right)\right] \tag{12}$$

Absorption model

The most common modeling of absorption cycle is based on the 1st Law of Thermodynamics, which refers to the conservation of mass and energy. The method discussed in the 2009 ASHRAE Handbook-fundamental is adopted in this study to model each component of the absorption cycle using Math-Cad program. Several assumptions and input parameters are required in order to model the entire component of the system [10]. These assumptions, listed in tab.1, are based on empirical and experimental results, and taken from the previously published works.

Table 1.Assumption for single-effect water/lithium bromide model

Assumptions
• The cycle is considered under steady state conditions.
• Refrigerant at outlets of both evaporator and condenser is saturated.
• Pressures at the generator and condenser are equal; pressures at evaporator and absorber are equal.
• Solutions exiting the absorber and the generator are saturated.
• The pump is considered under isentropic process.
• Expansion valves are considered under adiabatic process.
• Heat losses and pressure drops in the model components and tubes are negligible.

Based on the above set of assumptions, the analysis is carried out by applying mass and energy balance across each element of the absorption cycle in order to determine the rate of heat flows through the cycle, considering the order of energy flow shown in fig. 1.

The water vapor pressure is obtained in terms of evaporator and condenser temperatures (T_e , T_c) using the following equations [11]:

$$Pe = \mathrm{e}^{\left(\frac{C8}{Te} + C9 + C10 \cdot Te + C11 \cdot Te^2 + C12 \cdot Te^3 + C13 \cdot \ln(Te)\right)} \tag{13}$$

$$Pc = e^{\left(\frac{C8}{Tc} + C9 + C10 \cdot Tc + C11 \cdot Tc^2 + C12 \cdot Tc^3 + C13 \cdot \ln(Tc)\right)} \tag{14}$$

Since the refrigerant flowing through state points (1-4) of the cycle is the pure water refrigerant, the various enthalpies of the refrigerant at these state points can be obtained from the pure water properties data, knowing the state (saturated vapor/saturated liquid) and pressure of refrigerant. The equilibrium temperature and enthalpy of the LiBr/H_2O solution are defined by applying a multi-variable polynomial equation as function of the solution, refrigerant temperatures, T [°C], and solution concentration, X, through the absorber and generator unit, as given in Equilibrium Chart for Aqueous Lithium Bromide Solutions by the following equations [10]:

$$T = \sum_{0}^{3} b_n X^n + T_r \cdot \sum_{0}^{3} a_n X^n \tag{15}$$

$$h = \sum_{0}^{4} A_n X^n + T \sum_{0}^{4} B_n X^n + T^2 \sum_{0}^{4} C_n X^n \tag{16}$$

The actual performance of the cycle is measured by the coefficient of performance (COP), which is defined as the heat load in the evaporator per unit of heat load in the generator, and can be written as:

$$COP = \frac{Q_E}{Q_G} \tag{17}$$

Table 2.The various state points' properties for the single-effect LiBr/H2O absorption cycle presented in fig. 1

State point	State	Pressure	Temperature	Enthalpy	Mass flow rate	X
		[kPa]	[°C]	[kJ/kg]	[kg/s]	[% LiBr]
1	Superheated vapor	10.2	91.4	2671.0	0.209	0
2	Saturated liquid	10.2	46.2	194.0	0.209	0
3	Saturated liquid	0.82	4.12	194.0	0.209	0
4	Saturated vapor	0.82	4.12	2504.0	0.209	0
5	Weak solution	0.82	42.3	118.1	2.7	59.6
6	Weak solution	10.2	42.3	118.1	2.7	59.6
7	Weak solution	10.2	82.4	196.0	2.7	59.6
8	Strong solution	10.2	103.6	257.8	2.5	64.6
9	Strong solution	10.2	57.0	173.0	2.5	64.6
10	Strong solution	0.82	57.0	173.0	2.5	64.6
11	Chilled water	/	7	28.65	23.13	/
12	Chilled water	/	12	49.39	23.13	/
13	Cooling water	/	30	129.44	37.61	/
14	Cooling water	/	34	146.33	37.61	/
15	Cooling water	/	37.3	163.23	37.61	/
16	Hot water	/	108	453.31	26.41	/
17	Hot water	/	103	432.3	26.41	/

Solar fraction is the ratio of the useful energy provided by the solar system to the total heating energy required by the generator:

$$SF = \frac{Q_u}{Q_G} \tag{18}$$

The results of thermodynamic properties obtained for each state point of the absorption cycle corresponding to the 21st of July (at 4 pm) are presented in tab.2. It is considered that the outside wet bulb temperature is 25°C.

Results and Discussion

The mathematical model is an effective tool for predicting the performance of a water–LiBr solar assisted air conditioning system, and also for determining the heat and mass transfer at each component of the system. Since the main purpose of the solar-assisted air conditioning system is to meet the building cooling demands with low electricity consumption, the solar energy contribution to the total heat energy required for the generator is estimated. However, before evaluating all the system criteria, and for the purpose of accuracy, the model was studied in detail for the case adopted from ASHRAE [10]. The results obtained from the model were compared with the ASHRAE simulation results and they were found to be in a very good agreement with each other. Once the model was tested, the heat and mass transfer rates at each component of the absorption system and the system performance were calculated for the base case when there a 1000 m^2 of collector area was employed and 20° of collector's tilt angle.

The main influences on the system performance (COP) are the temperature levels in generator, solution concentration, condensing temperature and efficiency of solution heat exchanger SHX (Fig. 1). However, for the particular model of chiller considered in this study, optimizing these parameters could only improve the COP of the system very slightly. Generally, the average COP of the system remains almost constant at the average value of 0.7. As can be seen in fig. 3, to cover the seasonal cooling energy demand of nearly 637 MWh, for an average COP of 0.7, the system requires about 884 MWh of heating energy. The total heat of 302 MWh was delivered by solar collectors, while the remaining of about 582 MWh was supplied by an auxiliary heater (gas boiler). It means that the solar thermal system in this case is only capable of delivering the seasonal (April - September) average solar fraction of 34%, while the remaining 66% of thermal energy required by the absorption chiller has to be supplied by an auxiliary heating unit.

To achieve a higher solar fraction for the given cooling load profile, it is needed either to increase the area of collectors or to employ another type of solar collectors with a higher efficiency. Regardless the substitution of collector type, the surface area and the tilt angle of collectors were analyzed in order to reach the maximum solar fraction.

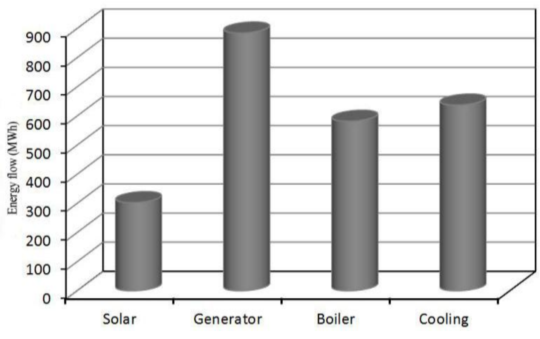

Figure 3. The seasonal energy flow

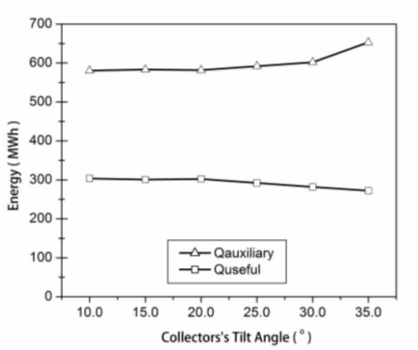

Figure 4. The effect of collector's tilt angle on the amount of useful and auxiliary energy

Regarding the tilt angle, the performance of solar collectors facing south was examined by varying the tilt angle from 10 to 35 degrees from horizontal position with an increment of 5°. The influence of collector's tilt angle variation on useful energy delivered and the auxiliary energy load for the entire cooling season are shown in fig. 4. The results indicate a slight difference in the required/obtained amount of energy between tilt angles (10-25). However, for tilt angle greater than 25, the auxiliary heater load is considerably increased. Hence the selected optimum angle for our study is 20°which is in very good agreement with the value suggested by Duffie and Beckman [12], who recommended that the slope of solar collectors for the solar cooling system should be equal to the latitude minus 15°. The effect of variation of collector area for the design day (21st of July) was analyzed under reference values of the other parameters. As expected, the absorbed heat through solar collectors is increased by increasing the collector area, which is indicated in fig.5(a, b, c and d). When 700 m^2 collector area is applied in the system, the share of solar energy and auxiliary heater to the total heating load required by the generator is 23% and 77% respectively. In the second case, when 1000 m^2 collector area is employed, solar energy share to the heating load requirement at generator has increased to 33%, while the auxiliary heater share decreased to 67%. In the third case, when 1200 m^2 collector area is employed, solar energy share to the heating load requirement has increased to 39%, while the auxiliary heater share decreased to 61%. In the last case, the use of 1400 m^2 collector area has increased the solar energy share to 48%, and decreased the auxiliary heater share to 52%.

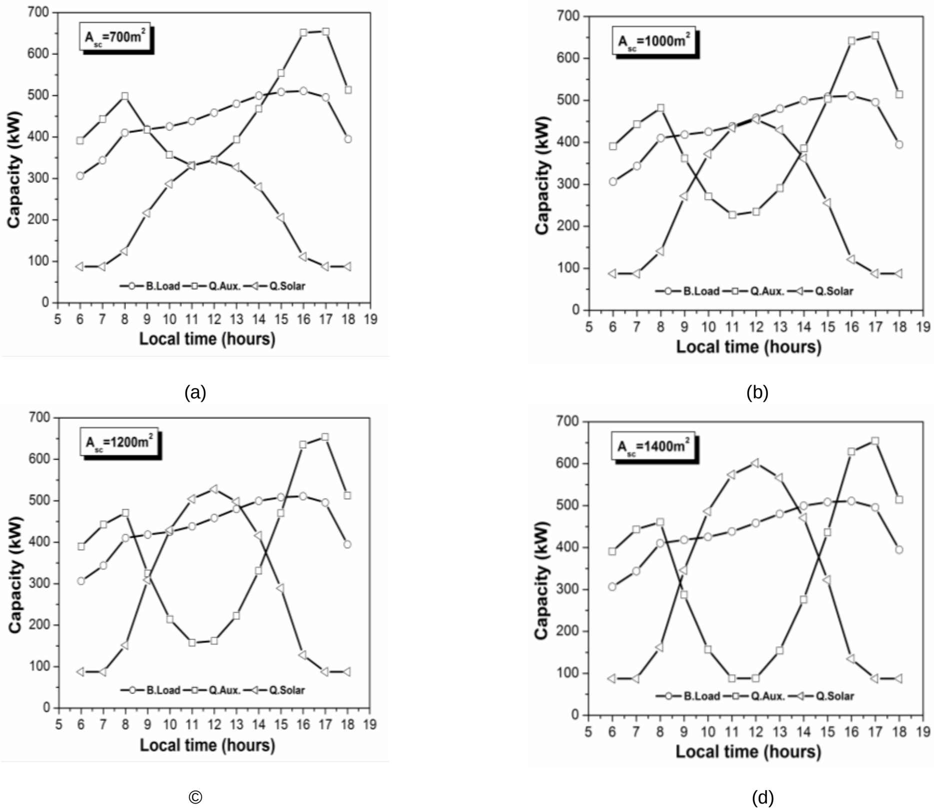

Figure 5.The effect of collector area

Additionally, in all cases of collector area variations it can be observed that the maximum cooling load has occurred in the afternoon hours, when the solar energy is not sufficient or not available (see fig. 6). Therefore, a large volume of hot water storage tank is essential to overcome this difficulty. However, in the case of 5-a (700 m^2) and 5-b (1000 m^2) there is no extra energy to be stored even at noontime with the highest incident solar radiation.

Fig. 7 presents the effect of collector area variation on the amount of energy delivered by the solar system and supplied by the auxiliary heater during the considered cooling season.

Moreover, besides the collector area, the main factors affecting the solar fraction are the local weather conditions (intensity of incident solar radiation) and the time of day when the plant is operated. According to the collector area analyses given in this paper only the case 5-d (1400 m^2) could provide a significant portion of the required heating energy. Though the available building's roof surface area is limited to 500 m^2, there are some possibilities to find an extra area for installing the additional 900 m^2 collector area, such as the parking place or the backyard of the building.

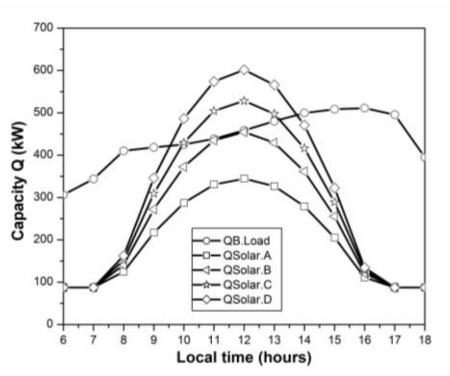

Figure 6. Building cooling load and solar gain for different collector area

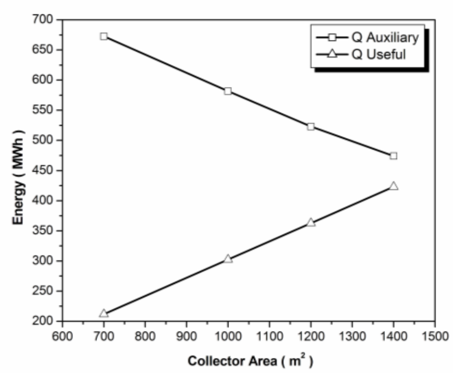

Figure 7. The amount of useful and auxiliary energy for different collector areas (April to September)

Comparing the base case (A_{sc} =1 000 m^2) with the last case (A_{sc} = 1400 m^2), an increase of about 14% in the amount of heat energy delivered by a solar collector system would be obtained in the latter case as shown in figs. (8 and 9). This is because in the latter case, the solar collector could provide nearly 423 MWh of driving heating energy required to cover the seasonal cooling load requirements, while the rest of about 461 MWh would be delivered by the auxiliary heater (gas boiler). This leads to an increase of the solar fraction to 48%, but the auxiliary heater fraction to be about 52%. It's clear that the heating energy consumed by the auxiliary heater is still quite high enough. To reach higher solar fraction, the surface area of collectors needs to be further increased. Though in this case the initial cost would be significantly higher, especially for solar collectors, there are many benefits from applying solar cooling system which need to be considered, including reducing CO_2 emissions, energy saving, reducing the operating cost *etc.*

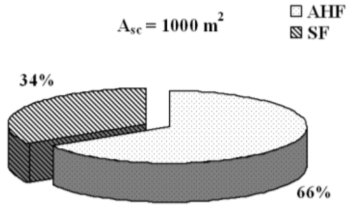

Figure 8. Seasonal solar fraction obtained by 1000 m^2 of collector area

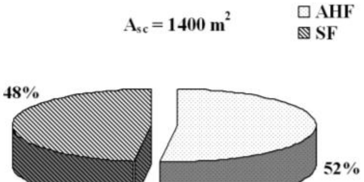

Figure 9. Seasonal solar fraction obtained by 1400 m^2 of collector area

Consequently, it's obvious that the area of solar collectors is the dominant parameter in increasing the solar fraction, especially in the specifications range considered for this study. On the other hand, solar collectors are considered to be the major component responsible for increasing the initial investment costs of the solar cooling systems. Hence, this study will be followed by an economic analysis for different collector surface area in order to determine the optimum surface area and to evaluate the economic viability of the whole system. In addition, another type of solar collector, which has higher efficiency as evacuated tubes, need to be tested and compare its effect on solar fraction with flat plate collector's results.

Conclusion

This paper presents a mathematical model of a flat-plate solar system coupled with a single-effect $LiBr/H_2O$ absorption chiller. The main objective of this study was to investigate the feasibility of solar assisted air conditioning system for an office building under Libyan climate conditions. Several analyses were carried out in order to estimate the total incident solar radiation on tilt surface. The total driving heating energy required for covering the cooling load demand during the whole season is about 884 MWh. A 302 MWh of this energy would be delivered by solar collectors, while the remaining of about 582 MWh would be delivered by an auxiliary heater (gas fired boiler).

The maximum solar fraction of 48% was obtained by means of 1400 m^2 of collector surface area. Analysis of the results indicates that, besides the collector surface area, the main factors affecting the solar fraction are the local weather conditions (intensity of incident solar radiation) and the time of day when the plant is operated.

Nomenclature

a, b, A, B,C	– constant coefficients, [-]
A_{sc}	– area of solar collector, [m^2]
C8 - C13	– constant coefficients, [-]
F'	– collector efficiency factor, [-]
FR	– heat removal factor, [-]
SR	– solar radiation absorbed by the collectors, [W/m^2]
H	– total radiation on horizontal surface, [J/m^2]
H_d	– daily horizontal diffuse radiation, [J/m^2]
I_b	– hourly beam radiation, [W/m^2]
I_d	– hourly diffuse radiation, [W/m^2]
I_{DN}	– direct radiation normal to the surface, [W/m^2]
I_{tts}	– total solar radiation, [W/m^2]
k_d	– daily diffuse solar fraction, [-]
LAT	– latitude, [°]
N	– number of day in the year, [-]
r_d	– ratio of hourly diffuse to daily diffuse radiation, [-]
G_{sc}	– solar constant (G_{sc}=1376 W/m^2)
T_{amb}	– ambient air temperature, [°C]
$T_{sol,in}$	– inlet water temperature of the Collector
UL	– overall heat transfer loss coefficient, [W/m K]

Greek symbols

β	– solar altitude angle, [°]
δ	– solar declination angle, [°]
Γ	– surface-solar azimuth angle, [°]
Σ	– tilt angle of collector from horizontal,[°]
ω_s	– sunset hour angle, [°]

References

[1] A. M. Mohamed, A. Habaibeh, H. Abdo, An investigation into the current utilization and prospective of renewable energy resources and technologies in Libya, Renewable Energy, 50 (2013), Feb, pp. 732-740.

[2] I.V. Luminosu et al. Research in solar energy at the Politechnica university of Timisoara: studies on solar radiation and solar collecors, Thermal science, 14 (2010) , 1, pp. 157–169.

[3] .E.M. Languri, et al. An energy and exergy study of a solar thermal air collector, Thermal science, 13, (2009), 1, pp. 205–216.

[4] K.F. Fong et al. Solar hybrid air-conditioning system for high temperature cooling in subtropical city, Renewable Energy, 35 (2010), 11, 2439-2451.
[5] Balghouthi M, Chahbani MH, Guizani A. Feasibility of solar absorption air conditioning in Tunisia, Building Environment, 43 (2008), 9, pp. 1459–70.
[6] A. Elsafty, A.J. Al-Daini. Economical comparison between a solar powered vapour absorption air-conditioning system and a vapour compression system in the Middle East, Renewable Energy, 25 (2002), 4, pp. 569–583
[7] Mazloumi M, Naghashzadegan M, Javaherdeh K. Simulation of solar lithium bromide–water absorption cooling system with parabolic trough collector, Energy Conversion and Management, 49 (2008), 10, pp. 2820–32.
[8] S. Ajib, W. Günther, Solar thermally driven cooling systems: Some investigation results and perspectives; Energy Conversion and Management 65 (2013), pp. 663–669.
[9] Duffie JA, Beckman WA. Solar energy thermal processes. New York: Wiley; 1974.
[10] ASHRAE Handbook of Fundamentals (SI). Chapters 2,6,14 and 20 (2009).
[11] S. A. Kalogirou, Solar thermal collectors and applications, Progress in Energy and Combustion Science, 30 (2004), 0, pp. 231-295.
[12] John A. Duffie, William A. Beckman, Solar Engineering of Thermal Processes, 3rd ed., John Wiley & Sons, Inc., 2006.

Paper submitted: December 29, 2012
Paper revised: February 21, 2013
Paper accepted: September 17, 2013